Distinct sets of $\alpha\beta$ TCRs confer similar recognition of tumor antigen NY-ESO-$1_{157–165}$ by interacting with its central Met/Trp residues

Laurent Derré[†‡], Marc Bruyninx[†‡], Petra Baumgaertner[†‡], Mathias Ferber[§¶], Daphné Schmid[§], Antoine Leimgruber[§¶], Vincent Zoete[¶], Pedro Romero[†], Olivier Michielin[§¶], Daniel E. Speiser[†‡], and Nathalie Rufer[‡§‖]

Divisions of [†]Clinical Onco-Immunology, Ludwig Institute for Cancer Research, and [§]Experimental Oncology, Multidisciplinary Oncology Center, Lausanne University Hospital, CH-1005 Lausanne, Switzerland; and [¶]Swiss Institute of Bioinformatics, Génopode, 1015 Lausanne, Switzerland

Communicated by Lloyd J. Old, Ludwig Institute for Cancer Research, New York, NY, August 14, 2008 (received for review November 27, 2007)

Naturally acquired immune responses against human cancers often include CD8$^+$ T cells specific for the cancer testis antigen NY-ESO-1. Here, we studied T cell receptor (TCR) primary structure and function of 605 HLA-A*0201/NY-ESO-$1_{157–165}$-specific CD8 T cell clones derived from five melanoma patients. We show that an important proportion of tumor-reactive T cells preferentially use TCR AV3S1/BV8S2 chains, with remarkably conserved CDR3 amino acid motifs and lengths in both chains. All remaining T cell clones belong to two additional sets expressing BV1 or BV13 TCRs, associated with α-chains with highly diverse VJ usage, CDR3 amino acid sequence, and length. Yet, all T cell clonotypes recognize tumor antigen with similar functional avidity. Two residues, Met-160 and Trp-161, located in the middle region of the NY-ESO-$1_{157–165}$ peptide, are critical for recognition by most of the T cell clonotypes. Collectively, our data show that a large number of $\alpha\beta$ TCRs, belonging to three distinct sets (AVx/BV1, AV3/BV8, AVx/BV13) bind pMHC with equal antigen sensitivity and recognize the same peptide motif. Finally, this in-depth study of recognition of a self-antigen suggests that in part similar biophysical mechanisms shape TCR repertoires toward foreign and self-antigens.

antigen recognition | cytolytic T lymphocytes | melanoma | T cell receptors | tumor immunity

The specificity of CD8$^+$ cytolytic T lymphocyte (CTL) responses relies on the interaction of clonotypically distributed antigen receptors (TCR) on the surface of the effector cell with small immunogenic peptide fragments displayed at the surface of a target cell by self-MHC class I molecules (pMHC) (1). Binding of the heterodimeric $\alpha\beta$-chains of the TCR to the pMHC complex is a key step leading to T cell activation and cell killing. The $\alpha\beta$ TCRs bind agonist pMHCs with relatively low affinity ($K_d \cong$1–100 μM) through complementary determining regions (CDR) present on their variable domains (2). The mature TCR repertoire is shaped by both positive and negative intrathymic selection, leading to an estimated 2.5×10^7 different TCR clonotypes in the human peripheral T cell pool (3). A relatively small number of CTL precursor cells is normally selected in response to the antigenic stimulus and comprises cells bearing several TCRs ($\approx$10 to $\approx$50 clonotypes) differing from each other yet having the ability to recognize the same pMHC complex. The recent development and availability of multimerized MHC–peptide complexes combined to TCR spectratyping with high-throughput DNA sequencing allowed the study of the development of antigen-driven CD8$^+$ T lymphocyte response to chronic antigenic exposure, e.g., in viral infection (CMV, EBV, HIV) or in cancer patients. The impact of TCR diversity on recognition of single antigenic pMHC complexes has been extensively investigated, and the relative contributions of each TCR β-chain have been addressed in several models. In a few systems, strong biases in the TCR repertoire selection of antigen-specific T cells, resulting in the preferential usage of particular $\alpha\beta$ TCR combinations, have been reported (4, 5) [supporting information (SI) *Text*].

Over the last 10 years, 24 class I and class II TCR–pMHC complexes have been crystallized and identified a substantial degree of structural variability in TCR–pMHC recognition (reviewed in ref. 6). In many cases, the TCR Vα interactions with the pMHC seem to predominate and, thus provide some basis for a conserved diagonal orientation of the TCR on the pMHC. Importantly, all aspects of TCR binding to pMHC have direct implications for TCR function. For instance, there is a direct link between peptide–MHC affinity and the efficiency of recognition by CD8$^+$ T lymphocytes (7), as similarly, there is a close relationship between the K_d of the TCR binding and the activity of the T cell in cytolytic assays (8, 9). Nevertheless, despite all of these efforts, the structural bases of TCR repertoire selection for pMHC complexes remain elusive.

The molecular recognition events taking place at the TCR–peptide–MHC interface are of great interest for medical applications. In particular, studies underlying pMHC recognition have important implications for the design of therapeutic antigen-based vaccines or of engineered TCRs. Therefore, the analysis of the primary structure of both α- and β-chains of the TCR, especially when combined with the functional analysis of the corresponding clonal populations of T cells, can provide important insights in TCR repertoire selection in response to a given pMHC ligand (10). Here, we report a detailed and combined molecular and functional characterization of the TCR repertoire specific for the cancer testis (CT) antigen NY-ESO-$1_{157–165}$ bound to HLA-A*0201, by the analysis of large numbers of T cell clones and TCRs derived from melanoma patients with naturally occurring CD8$^+$ T cell responses.

Results

Naturally Occurring NY-ESO-$1_{157–165}$-Specific CD8$^+$ T Cell Responses Display a Preferential Usage of BV1, BV8, and BV13 TCRs. Previous studies have focused much attention on tumor antigens encoded by cancer germ-line genes, whose expression can be found in various types of tumors but not in normal adult tissues, with the exception of testis. In particular, because of its frequent expression in tumors and immunogenicity in advanced cancer patients, NY-ESO-1 is currently viewed as an ideal candidate for thera-

Author contributions: P.R., D.E.S., and N.R. designed research; L.D., M.B., P.B., M.F., D.S., and N.R. performed research; A.L., V.Z., and O.M. contributed new reagents/analytic tools; L.D., M.F., O.M., D.E.S., and N.R. analyzed data; and D.E.S. and N.R. wrote the paper.

The authors declare no conflict of interest.

[‡]L.D., M.B., P.B., D.E.S., and N.R. contributed equally to this work.

[‖]To whom correspondence should be addressed at: Multidisciplinary Oncology Center (CePO), Hôpital Orthopédique, Niveau 5, Aile Est, Avenue Pierre-Decker 4, CH-1005 Lausanne, Switzerland. E-mail: Nathalie.Rufer@unil.ch.

This article contains supporting information online at www.pnas.org/cgi/content/full/0807954105/DCSupplemental.

peutic tumor antigen-based vaccines. Recently, we reported an unusually strong natural tumor-specific immune response against NY-ESO-$1_{157–165}$ in patient LAU 50 with advanced melanoma (11), characterized by expansions of codominant T cell clonotypes bearing distinct BV1, BV8, or BV13 TCRs (12). These data prompted us to examine the proportion of BV1, BV8, and BV13 TCRs present within NY-ESO-1-specific T cells of peptide-stimulated PBMCs from four additional melanoma patients with naturally occurring NY-ESO-1-specific CTL responses (13). By using HLA-A2/NY-ESO-$1_{157–165}$ multimers in combination with mAbs directed against the variable region of TCR BV1, BV8, and BV13, we found that the majority of multimer$^+$ T cells expressed TCRs with these BV elements (Fig. S1), in line with a recent report by Le Gal and colleagues (10).

Restricted CDR3β Diversity and High Sequence Homology Among NY-ESO-1-Specific TCRs Bearing the TCR BV8 Gene Segment. Using an approach that combines flow cytometry based-cell sorting, TCR spectratyping, and sequencing at the single cell level, we recently identified, in a single patient (LAU 50), nine codominant NY-ESO-1-specific T cell clonotypes characterized by distinct BV1, BV8, or BV13 TCRs sequences (12). Extensive studies of their clonal composition revealed a high degree of sequence homology of the NY-ESO-1-specific TCRs bearing the TCR BV8 gene segment (Fig. S2). These data prompted us to examine in great detail 605 NY-ESO-1-specific T cell clones generated *in vitro* from patients LAU 50, LAU 97, LAU 155, LAU 156, and LAU 198 (Fig. S1). Complete TCR analysis by sequencing allowed the identification of a total of 49 NY-ESO-1-specific clonotypes, classified into BV1 (12 times), BV8 (21 times), or BV13 (16 times) TCR usage (Fig. 1), including the nine characterized clonotypes from patient LAU 50 (12). A striking feature was that, with two exceptions, all BV8-expressing NY-ESO-1-specific clonotypes shared the same relatively short length of the β-chain CDR3 region (7 aa). Moreover, there was a preferential usage of either the BJ1S1 or the BJ2S1 gene segments and a marked conservation of the CDR3 amino acid composition, particularly at positions 3, 6, and 7 with prominent usage of a glycine, a glutamate, and a glutamine residue, respectively. Interestingly, the TCR analysis of BV1- and BV13-specific T cell clones yielded different results. Indeed, despite conserved BV usage, most of these clonotypes used different BJs and different CDR3β loop sequences of highly variable lengths ranging from 6 to 13 aa (Fig. 1).

BV8 T Cell Clonotypes Pair with a Highly Restricted Set of Vα-Chains in Contrast to the BV1 and BV13 NY-ESO-1-Specific T Cell Clonotypes. To assess the full extent of conservation of the primary TCR structure of the BV8 T cell clonotypes, we next examined the TCR α-chain clonal diversity and junctional features of the 20 NY-ESO-1-specific T cell clones defined as dominant clonotypes based on their frequencies, implying that at least three individual T cell clones share the identical TCR β-chain sequence (Fig. 1). Strikingly, sequencing of the complementary TCR α-chains demonstrated the highly recurrent usage of the AV3S1 gene segment by all BV8S2 T cell clonotypes (Fig. 2). Moreover, we observed a marked conservation of the V(D)J junctional sequences and a unique CDR3α length (6 aa) within clonotypes derived from the same and distinct patients. Aside the preferential usage of the AJ31 gene segment, the dominant NY-ESO-1-specific T cell clonotypes were also characterized by their preferred selection of aspartate/leucine at CDR3α positions 1/6, respectively. In sharp contrast, the Vα repertoires associated with both BV1 and BV13 TCRs were highly heterogeneous and comprised various AJs and various CDR3α lengths ranging from 7 to 14 aa (Fig. 2).

	Patient	BV	CDR3	BJ	# clones
			1 2 3 4 5 6 7 8 9 10 11 12 13		
	LAU 50	BV1	T S S G A N V L	2S6	1
1	LAU 50	BV1S1	S V T G T G G G	2S1	61
2	LAU 50	BV1S1	S V T G T E E A	1S1	6
3	LAU 50	BV1S1	S V D G S N Q P Q	1S5	10
4	LAU 155	BV1S1	S V A T G G D T Q	2S3	29
	LAU 50	BV1	S V P G D T D T Q	2S3	1
	LAU 50	BV1	S L A H L G E T Q	2S5	1
5	LAU 155	BV1S1	S L A T G G D T Q	2S3	5
	LAU 50	BV1S1	S P T Q E G Y S P L	1S6	2
	LAU 50	BV1S1	S P E E G R T D T Q	2S3	2
	LAU 50	BV1	S V A G D I Q E T Q	2S5	1
	LAU 50	BV1	S S Q G G G G T R Q	2S7	1
	LAU 50	BV8S2	S R T G E V	2S7	2
	LAU 50	BV8	S F R Q E T Q	2S5	1
	LAU 97	BV8	S F H T D T Q	2S3	1
	LAU 155	BV8	S Q G A N V L	2S6	1
	LAU 155	BV8	S L G A G E A	1S1	1
6	LAU 50	BV8S2	S L G G T E A	1S1	29
7	LAU 50	BV8S2	S L G G N E Q	2S1	9
8	LAU 155	BV8S2	S L G S T E A	1S1	20
	LAU 97	BV8	L L A A G E L	2S2	1
9	LAU 50	BV8S2	Q Q G G T E A	1S1	96
10	LAU 50	BV8S2	K Q G G N E Q	2S1	4
11	LAU 156	BV8S2	K G G A N E Q	2S1	31
	LAU 50	BV8	K P G A G E Q	2S7	1
12	LAU 155	BV8S2	N S G A N E Q	2S1	3
13	LAU 155	BV8S2	N S G S N E Q	2S1	11
	LAU 50	BV8	N Q G A Q P Q	1S5	1
	LAU 155	BV8	N T G A N E Q	2S1	1
	LAU 155	BV8	R K G P N E Q	2S1	1
	LAU 50	BV8	R P A G Q P Q	1S5	1
	LAU 50	BV8	R V G A D T Q	2S3	1
	LAU 50	BV8	S L D R A T N E K L	1S4	1
14	LAU 155	BV13S1	L K G L T Q	2S5	7
15	LAU 50	BV13S1	R T G L D G Y	1S2	135
	LAU 50	BV13	A P R E N Y G Y	1S2	1
	LAU 50	BV13	S P T G F N E Q	2S1	1
	LAU 50	BV13	S Y S G V Q E T Q	2S5	1
16	LAU 155	BV13S1	S Y V G A A G E L	2S2	6
	LAU 50	BV13	S Y R G G S E T Q	2S5	1
17	LAU 50	BV13S1	S Y V G G K A E A	1S1	77
18	LAU 198	BV13S1	S Y E A G A E T Q	2S5	21
	LAU 50	BV13	S S K L V G E T Q	2S5	1
	LAU 50	BV13	R D R Q A N Y E Q	2S7	1
19	LAU 50	BV13S6	S L T G H Y N S P L	1S6	6
20	LAU 155	BV13S6	S L T G G L N S P L	1S6	5
	LAU 155	BV13	S Y Q G G G K N T E A	1S1	1
	LAU 155	BV13S6	L G D G D G A Y N S P L	1S6	2
	LAU 156	BV13S2	S R D S A L W I S T D T Q	2S3	2

Fig. 1. Sequence analysis of TCR junctional transcripts derived from BV1$^+$, BV8$^+$, and BV13$^+$ NY-ESO-$1_{157–165}$ multimer$^+$ T cell clones from five melanoma patients. Transcripts were reverse-transcribed and amplified from multimer$^+$ T cell clones by using either pairs of BV1/BC, BV8/BC, or BV13/BC primers. PCR products were directly purified and sequenced. Conserved residues forming the CDR3 loop and preferential BJ gene element usages are highlighted in gray. The number of *in vitro* generated T cell clones displaying a given sequence is depicted. Of note, the NY-ESO-1-specific CD8$^+$ T cell response seen in patients LAU 156 and LAU 198 was composed of, respectively, a single dominant BV8 and BV13 T cell clonotype, confirming the results obtained by using anti-BV antibodies and flow cytometry (Fig. S1).

Similar Efficient Tumor Cell Recognition and Killing by NY-ESO-1-Specific T Cell Clones with Distinct Primary TCR Structures. To evaluate the relationship between the NY-ESO-1-specific T cell clonotypes and functional avidity for antigen recognition, 82 T cell clones generated from patient LAU 50, distributed according to their TCR BV1, BV8, or BV13 clonotypic expression, were assessed in chromium release assays for their ability to recognize graded concentrations of the native NY-ESO-$1_{157–165}$ peptide pulsed to T2 cells (Fig. 3). Remarkably,

	Clonotype ID	BV	CDR3	BJ	AV	CDR3	AJ
			1 2 3 4 5 6 7 8 9 10 11 12 13			1 2 3 4 5 6 7 8 9 10 11 12 13 14	
1	*LAU 50-clono1	BV1S1	S V T G T G G G	2S1	AV25S1	Y M D S N Y Q L	33
2	LAU 50-clono3	BV1S1	S V T G T E E A	1S1	AV6S1	P Y S F S G G Y N K L	4
3	LAU 50-clono2	BV1S1	S V D G S N Q P Q	1S5	AV4S1	R K T S Y D K V	50
4	*LAU 155-clono1	BV1S1	S V A T G G D T Q	2S3	AV2S1	P Y S G A G S Y Q L	28
5	LAU 155-clono2	BV1S1	S L A T G G D T Q	2S3	AV2S1	N K A S G N T P L	29
6	LAU 50-clono2	BV8S2	S L G G T E A	1S1	AV3S1	D A E A R L	31
7	LAU 50-clono3	BV8S2	S L G G N E Q	2S1	AV3S1	D G E S R L	58
8	LAU 155-clono2	BV8S2	S L G S T E A	1S1	AV3S1	D G D A R L	31
9	*LAU 50-clono1	BV8S2	Q Q G G T E A	1S1	AV3S1	D K N A R L	31
10	LAU 50-clono4	BV8S2	K Q G G N E Q	2S1	AV3S1	D G V G K L	23
11	*LAU 156-clono1	BV8S2	K G G A N E Q	2S1	AV3S1	D E S A R L	31
12	LAU 155-clono3	BV8S2	N S G A N E Q	2S1	AV3S1	D G N A R L	31
13	*LAU 155-clono1	BV8S2	N S G S N E Q	2S1	AV3S1	D E W G K L	23
14	LAU 155-clono2	BV13S1	L K G L T Q	2S5	AV3S1	D A S Y G Q N F	26
15	*LAU 50-clono1	BV13S1	R T G L D G Y	1S2	AV14S1	S D S N Y Q L	33
16	LAU 155-clono1	BV13S1	S Y V G A A G E L	2S2	AV23S1	R P Q T G G S Y I P	6
17	*LAU 50-clono2	BV13S1	S Y V G G K A E A	1S1	AV23S1	R S S M D S N Y Q L	33
18	LAU 198-clono1	BV13S1	S Y E A G A E T Q	2S5	AV6S2	R E G P S G G G T S Y G K L	52
19	LAU 50-clono3	BV13S6	S L T G H Y N S P L	1S6	AV2S1	G G G A N N L	36
20	LAU 155-clono3	BV13S6	S L T G G L N S P L	1S6	AV7S2	T V D S N Y Q L	33

Fig. 2. Junctional amino acid sequence of TCR α-chains associated with each TCR β transcript derived from dominant NY-ESO-$1_{157–165}$-specific T cell clonotypes. Conserved residues forming the CDR3α/β loops and preferential AJ/BJ gene element usages are highlighted in gray. *, Clonotypes recently described in ref. 10.

most of the BV1-, BV8-, and BV13-derived clonotypes showed similar functional avidity because 50% maximal lysis of T2 cells was found at similar peptide doses ($10^{-9}/10^{-10}$ M). One exception was BV13 clonotype 2 that exhibited a slightly but statistically significant inferior functional avidity of antigen recognition compared with the other tested clonotypes. Lysis of targets sensitized with an analog peptide with a C to A substitution at peptide position 9 was achieved at ≈1 log lower peptide concentrations ($10^{-10}/10^{-11}$ M), which corresponds to the increased pMHC stability (14). The ability of the BV1, BV8, and BV13 clonotypes to specifically lyse NY-ESO-1-expressing tumor cell lines revealed that all distinct T cell clonotypes efficiently and similarly recognized the NY-ESO-1-expressing melanoma cell lines Me 275 and Me 290 (Figs. S3 and S4). Altogether, our results demonstrate that T cells bearing three distinct sets of $\alpha\beta$ TCRs (AVx/BV1S1, AV3S1/BV8S2, or AVx/BV13) shared similar avidity for antigen recognition and tumor reactivity, irrespective of their BV usage.

Both Met and Trp Residues Located in the Middle Region of the Antigenic Peptide Are Critical TCR Contact Residues Regardless of TCR Gene Segment Usage. To gain information about the specific role of each single amino acid of the NY-ESO-1 peptide in the interaction with well defined TCRs, we analyzed the cytotoxicity of 11 BV1, BV8, and BV13 molecularly defined T cell clonotypes against T2 cells loaded with a set of NY-ESO-$1_{157–165}$ single alanine-substituted peptide variants. The recognition patterns of each codominant clonotype are depicted in Fig. 4*A*. The relative antigenic activity was calculated by using the native peptide NY-ESO-$1_{157–165}$ as reference. As described (13, 14), the peptide with the C165A replacement appeared to be the most efficient antigenic peptide analog, improving HLA-A2 binding and resulting in a marked increase in the recognition by every clonotype. All four BV8 clonotypes exhibited a more homogeneous pattern of fine specificity of recognition compared with the recognition patterns found for BV1 and BV13 T cell clones. Strikingly, several amino acid residues located in the middle region of the antigenic peptide (P3–P8) appeared critical for the recognition by BV1, BV8, or

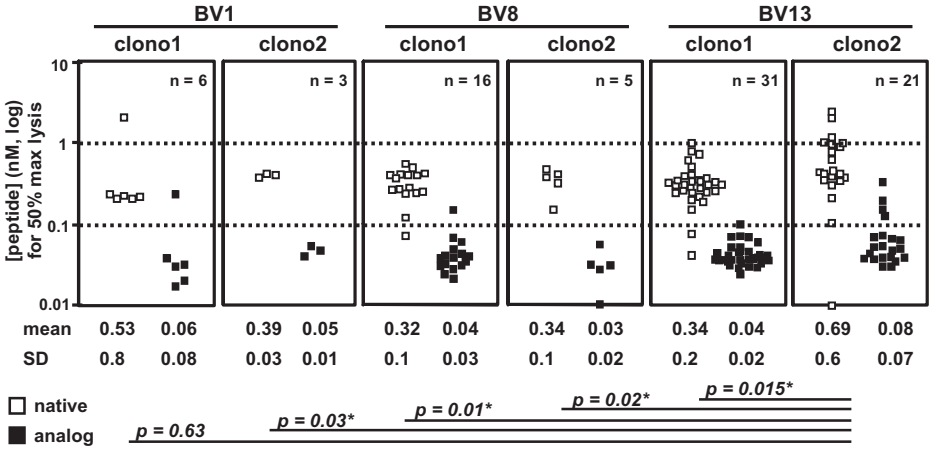

Fig. 3. Fine specificity of NY-ESO-1 antigen recognition of tumor-reactive T cell clones derived from patient LAU 50. The relative TCR functional avidity was compared by using T2 target cells (HLA-$A2^+$/$TAP^-/^-$) pulsed with graded concentrations of either the native NY-ESO-$1_{157–165}$ peptide (SLLMWITQC) or the analog NY-ESO-$1_{157–165}$ peptide (SLLMWITQA). Complete collection of data (n = 82 clones) representing the peptide concentration (either native or analog) used to achieve 50% of maximum lysis is shown. Each data point represents the result of an individual clone. Mean ± SD values (nanomolar) are shown. *, $P \leq 0.03$ with the Welch two-sample t test.

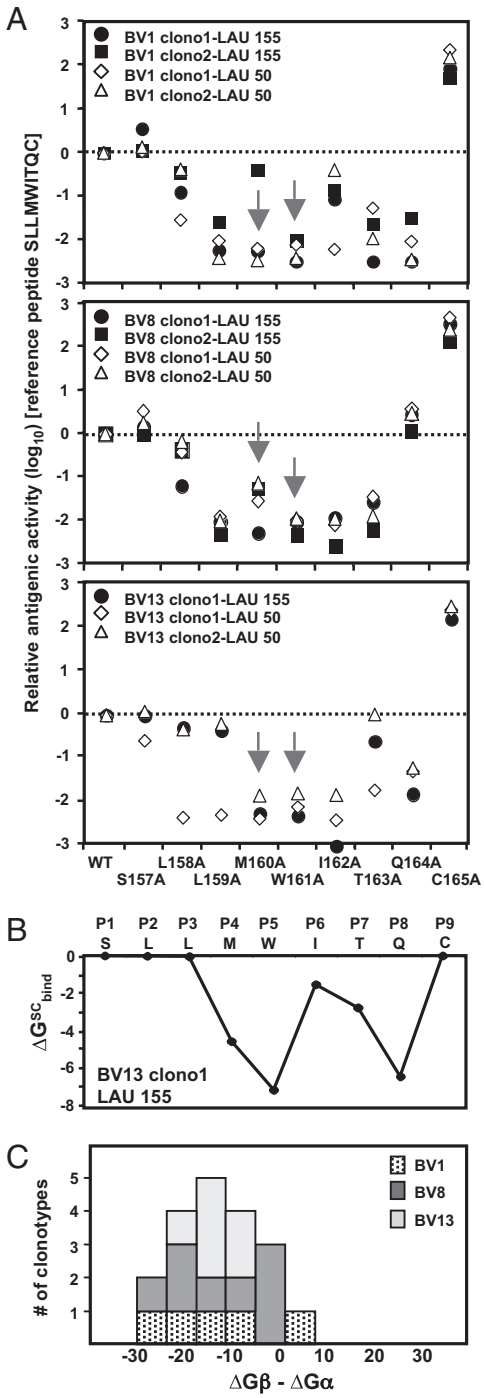

Fig. 4. Contribution of individual NY-ESO-$1_{157–165}$ amino acid residues to functional antigen recognition by specific T cell clonotypes. (*A*) The relative antigenicity of alanine-substituted NY-ESO-1 peptide analogs was assessed on T2 target cells in the presence of graded peptide concentration. We used five and six distinct T cell clonotypes (BV1, BV8, and BV13) isolated from patients LAU 155 and LAU 50, respectively. The molar concentration required for 50% maximal lysis by each T cell clone and for each peptide was calculated from peptide titration experiments. The relative antigenic activity of each peptide analog was determined by using the native peptide NY-ESO-1 as a reference (*SI Text*). The recognition patterns of BV1-, BV8-, and BV13-derived clonotypes are depicted in separate panels of graphs. (*B*) Estimation of the binding free energy contributions of each residue of the NY-ESO-$1_{157–165}$ peptide for the TCR BV13 clonotype 1 isolated from patient LAU 155. Of note, the side chains of the central residues (P4–P8) showed important favorable contributions in the binding between peptide and TCR, whereas the contributions of the outer side chains (P1, P2, P3, and P9) were not significant. (*C*) Comparison of the sum of the binding free energy contributions made by the TCR Vβ residues and the TCR Vα residues toward the HLA-A*0201/NY-ESO-$1_{157–165}$ complex. Histogram count of 19 of the 20 TCR models was generated *in silico*, as a function of the $\Delta G_{\beta,\text{bind}} - \Delta G_{\alpha,\text{bind}}$ difference. The $\Delta G_{\beta,\text{bind}} - \Delta G_{\alpha,\text{bind}}$ difference is in kilocalories per mole. Of note, the 2BNR (15) $\Delta G_{\beta,\text{bind}} - \Delta G_{\alpha,\text{bind}}$ difference was −6.4 kcal/mol, conferring again a preponderant role to the β-chain in the binding process.

BV13 T cell clonotypes. Both methionine (P4) and tryptophan (P5) residues were particularly crucial for their interaction with the TCR, as demonstrated by the low recognition by all of the BV1, BV8, and BV13 clonotypes for the peptides containing M160A and W161A substitutions (Fig. 4*A*). Finally, other residues (Leu-P3, Ile-P6, Thr-P7, and Gln-P8) were highly critical for only some but not other clonotypes (either BV1, BV8, or BV13). The contributions of the side chains of the NY-ESO$_{157–165}$ peptide to the binding free energy of the BV13 clonotype 1 from patient LAU 155 were calculated according to the Molecular Mechanics–Generalized Born Surface Area (MM-GBSA) approach (Fig. 4*B* and *SI Text*) and are in good agreement with the functional recognition pattern found for the same clonotype (Fig. 4*A*). This particular clonotype was chosen because of the availability of a very closely related TCR–pMHC x-ray structure, designated as the 2BNR complex (15).

Prevalent Contribution of the TCR β-Chain for the Binding Free Energy Toward the NY-ESO-$1_{157–165}$/HLA-A*0201 Complex. The *in silico* modeling of the TCR–pMHC was performed for the 20 dominant NY-ESO-1-specific T cell clonotypes. For each model and for the 2BNR structure (15), we calculated side chains and backbone contributions to the binding free energy made by the TCR residues (*SI Text*). Fig. 4*C* shows a histogram count of the models, as a function of the $\Delta G_{\beta,\text{bind}} - \Delta G_{\alpha,\text{bind}}$ difference. Except for BV1-clono2 (LAU 155) TCR, a large majority of models showed a preferential β-chain contribution (i.e., a negative $\Delta G_{\beta,\text{bind}} - \Delta G_{\alpha,\text{bind}}$ difference), revealing its greater importance compared with the α-chain, in the binding with NY-ESO peptide and MHC complex.

Discussion

In the present work, we performed a detailed analysis of primary structure and function of the TCR $\alpha\beta$ repertoire toward the immunodominant HLA-A2/NY-ESO-$1_{157–165}$ epitope. The analysis of a large number of T cell clones (605 clones) showed that an important proportion of tumor-reactive CD8$^+$ T lymphocytes preferentially expressed the TCR AV3S1-BV8S2 chains with a remarkably high degree of conservation of CDR3α and β domains, in terms of both length and amino acid composition at certain positions. These data are further emphasized by the comparable recognition patterns of fine specificity exhibited by distinct AV3/BV8 T cell clonotypes, as revealed by the experiments using a set of single alanine-substituted NY-ESO-1 peptides. Collectively, this report demonstrates that similarly to the CD8$^+$ T cell responses observed against viral influenza A matrix protein and EBV EBNA3 epitopes (4, 5), highly restricted and conserved TCR $\alpha\beta$ usage can also be observed in CTL responses toward self/tumor antigens such as NY-ESO-1.

Another major finding is that besides the selected AV3S1/BV8S2 set of T lymphocytes, NY-ESO-1-specific TCR repertoires were biased toward the usage of BV1 and BV13 gene segments. However, in contrast to the AV3S1/BV8S2 set, the BV1 and BV13 TCR sets revealed corresponding Vα repertoires of high diversity. Overall, these TCR α-chains were characterized by different Vα and Jα usage of highly variable CDR3 length and amino acid composition. Similar to our data, a recent study showed that CTL specific for the protective immunodominant nucleoprotein epitope (NP366–374) of influenza A viruses in B6 mice used a highly restricted Vβ repertoire but no conserved Vα

repertoire (16). Despite the limited set of human T cell clones analyzed, similar conclusions were reached by another study based on HIV-specific CTL responses from long-term survivors (17). Altogether, these observations reveal an unsuspected diversification of the TCR $\alpha\beta$ repertoire, which would have been qualified as "highly restricted" had such analyses remained limited to the TCR β-chain repertoire. Therefore, TCR repertoire studies need to include the characterization of both TCR α- and β-chains and not only the latter as done in the majority of previous studies.

Because NY-ESO-1-specific T cells expressed biased TCR BV1 and BV13 chains but can use a variety of TCR α-chains, our data suggest that recognition of the NY-ESO-$1_{157-165}$/HLA-A*0201 complex may predominantly depend on the TCR β-chain. In this regard, the *in silico* modeling of the NY-ESO-1-specific T cell repertoire combined with the MM-GBSA decomposition of the binding free energy into TCR α and β contributions revealed that a large majority of specific T cell clonotypes have a preferential β-chain contribution to the TCR–pMHC binding compared with their corresponding α-chain. Collectively, our finding emphasizes the prevalent role of the β-chain in contributing to more favorable interactions with the pMHC ligand than the α-chain. Curiously, the results described here and in the above-mentioned studies do not exactly recapitulate those found by others that rather suggest a predominant role of TCR α-chain in determining the preimmune repertoire of antigen-specific T cells (18–20). In line with this view, Yokosuka *et al*. (18) have investigated the potential spectrum of TCR $\alpha\beta$-chains to exhibit antigen specificity by systematically analyzing hundreds of individual TCR $\alpha\beta$ pairs for antigen-specific recognition. Their findings show that to recognize the HIVgp160 peptide/H-2Dd complex, CTLs have to possess a single TCR α-chain but can use a variety of TCR β-chains. Restricted α-chain usage (i.e., Vα2.1) was also found among HLA-A2/Melan-A specific T cells (19, 20). Consistent with these results, Miles *et al*. (21) have recently shown that MHC restriction in the $CD8^+$ T cell response to an epitope from EBV, which is naturally immunogenic across two human MHC class I alleles, can be controlled exclusively by TCR α-chain usage.

Many self-antigens are expressed in the thymus (22), associated with negative selection of T cells expressing specific TCRs, in some instances explaining why self/tumor antigen-specific TCRs are of lower avidity as opposed to pathogen-specific TCRs (2). For example, the self/tumor antigen Melan-A/MART-1 is recognized by relatively low avidity TCRs, and these TCRs present higher degrees of TCR β-chain heterogeneity (23). Although avidities of the HLA-A2/NY-ESO-1 specific TCRs are somewhat higher, they still do not reach the high avidities observed among virus-specific TCRs. Nevertheless, the majority of $HLA\text{-}A2^+$ individuals are capable of mounting vigorous CD8 T cell responses to this antigen, confirming that it is a preferential target of tumor-specific T cells. Thus, one could speculate that the TCR repertoire studied here is not (much) impaired by thymic negative selection. The question remains open whether similar observations as shown here for NY-ESO-1-specific TCRs can be made for TCRs specific for other self/tumor antigens.

What remains intriguing, at present, is which biophysical mechanisms allow TCRs that either display highly conserved Vα- and β-chains or semiconserved Vβ-chains pairing with complementary diverse Vα-chains, to recognize the same pMHC complex. Despite the 24 solved structures of TCRs–pMHC complexes (6), many of the structural principles that govern MHC restriction still remain unclear. The crystal of the influenza MP_{58-66}/HLA-A2-specific TCR AV10S2/BV17 provides some structural explanations for the specific contribution of BV17 (24). Indeed, the distinctive orientation of this TCR, which is almost orthogonal to the peptide-binding groove of HLA-A2, facilitates insertion of a conserved arginine in the Vβ CDR3 into a notch between the bound peptide and the MHC α2-helix. This unusual interaction may compensate for the lack of prominent side chains of the Flu-peptide pointing toward the TCR (25). Further insights in the comparison of reported TCR–pMHC crystal structures reveal that TCR binding generally occurs in a flexible diagonal orientation to the long axis of the MHC peptide-binding groove (6). Class I MHC molecules usually bind peptides of 8–10 residues in length (on average 9 mers defined as P1–P9) in an extended conformation in which the peptide is fixed at its ends by pockets formed by the MHC molecule. In contrast, the centrally located peptide residues exhibit upward-pointing amino acid side chains that often interact directly with TCR CDR3 loops (6).

Because the NY-ESO-1/A2 complex preferentially selects and binds to (*i*) conserved AV3S1/BV8S2 and (*ii*) semiconserved AVx/BV1 and AVx/BV13 TCRs, this antigenic model provides us with the unique opportunity to examine in detail the biophysical nature of distinct TCRs recognizing the same pMHC ligand and the impact of each TCR α- and β-chain on such recognition. Our functional data, using a panel of NY-ESO-$1_{157-165}$ single alanine-substituted peptide variants, revealed the critical role played by two central residues, Met-P4 and Trp-P5, for the antigenic recognition by different T cell clonotypes. The work reported here confirms and further extends the results obtained from the crystal structure of the 2BNR complex, indicating that binding of the TCR centers on two prominent side chains of the two central amino acids, methionine–tryptophan (15), forming a predominant hot spot interacting with the CDR3α and β loops (26). Because our observations were made on an extended pool of dominant T cell clonotypes isolated from two different patients (LAU 50 and LAU 155), they indicate that this represents a general feature, i.e., that distinct TCRs (AVx/BV1, AV3S1/BV8S2, AVx/BV13) share comparable peptide recognition patterns, suggesting conserved binding modes of distinct A2/NY-ESO-1 specific TCRs. In particular, preliminary observations on *in silico* models suggest that some conformational motifs within the CDR3β loop may be critical for the binding to the NY-ESO-$1_{157-165}$ peptide (data not shown). The issue of which residues within the CDR1, CDR2, and CDR3 α and β loops present dominant contributions to (*i*) antigen recognition and (*ii*) MHC recognition deserves additional studies combining detailed structural and functional investigations.

A better understanding of structural principles that govern TCR recognition is essential to promote research and clinical applications. The quality of TCRs recruited during disease, or by vaccination, dominantly influences the potency of immune responses (27). To improve therapeutic immune interventions, TCRs need to be fully characterized, and the mechanisms for their recruitment and function must be elucidated. Results from such studies impact, e.g., on the design of antigens for vaccination and on the choice of optimal TCRs for adoptive T cell therapy, with or without TCR gene transfer. Here, we show that the TCR β-chain, comparable with the TCR α-chain in other models, may play an important role in the recognition of pMHC complexes and that depending on the pMHC model, each chain may present dominant contributions to antigen recognition. In addition, similar mechanisms may control TCR repertoire shaping toward foreign or self-antigens because the predominant contribution of the TCR α- or β-chain can be observed under various physiopathological contexts, e.g., acute or chronic *in vivo* triggering by either viral or tumor antigens. Finally, our data demonstrate that three distinct sets of TCRs (AVx/BV1, AV3/BV8, and AVx/BV13) are able to recognize the same NY-ESO-1/MHC complex with comparable and high functional avidity, conferring successful tumor recognition.

Materials and Methods

Patients, Cell Preparation, and Flow Cytometry. Five HLA-A*0201 melanoma patients (LAU 50, LAU 97, LAU 155, LAU 156, and LAU 198) provided written informed consent and thus participated in this study of the Ludwig Institute for Cancer Research (LICR) and of the Multidisciplinary Oncology Center, which was approved by Institutional Review Boards and the LICR Protocol Review Committee. Samples were collected and processed for peptide stimulation experiments and for HLA-A2/peptide multimer staining as described in the *SI Text*.

Generation of T Cell Clones and Functional Cytolytic Assays. Multimer^{pos} CD8^{pos} T cells were sorted in a FACSVantage SE machine (Becton Dickinson) and cloned by limiting dilution and expanded as described in the *SI Text*. The functional avidity of antigen recognition was analyzed for *in vitro* generated T cell clones, isolated from patients LAU 50 and LAU 155, and bearing molecularly defined $\alpha\beta$ TCR clonotypes as detailed in the *SI Text*.

TCR-BV and -AV Repertoire Analysis. TCR-BV and -AV repertoire analysis was performed after spectratyping, sequencing, and clonotyping as detailed in the *SI Text*.

Binding Free Energy Calculations. The estimation of the binding free energy contributions of each residue of the NY-ESO-1 peptide to the TCR–pMHC association was performed on the TCR BV13 clonotype 1 from LAU 155, which is highly related to the TCR AV23-BV13 (1G4) bound to NY-ESO-1$_{157–165}$/HLA-A*0201 (15), as described in the *SI Text*.

Computational TCR Modeling. To calculate the binding free energy contributions made by the TCR Vα and Vβ residues, homology models of the variable domain of the TCR bound to the SLLMWITQC peptide presented by HLA-A*0201 were built by using Modeler 6v2 (28), based on the 2BNR complex (15) and other crystal structures of TCR from the Protein Data Bank (*SI Text*).

ACKNOWLEDGMENTS. We acknowledge our patients for active participation and the hospital staff for excellent collaboration. We thank J.-C. Cerottini, V. Jongeneel, D. Kuznetsov, S. Leyvraz, D. Liénard, D. Rimoldi, C. Servis, B. Stevenson, and V. Voelter for collaboration and advice; E. Devevre for cell sorting; and I. Luescher and P. Guillaume (Ludwig Institute for Cancer Research, Lausanne, Switzerland) for multimers. We also thank the excellent technical and secretarial help of P. Corthesy-Henrioud, C. Geldhof, R. Milesi, D. Minaïdis, N. Montandon, and M. van Overloop. This work was sponsored and supported by the Swiss National Center of Competence in Research (NCCR) in Molecular Oncology, the Ludwig Institute for Cancer Research, the Cancer Research Institute, New York, and Swiss National Science Foundation Grants 3100A0-105929 and 3200B0-107693. P.R. was supported by the European Union FP6 Cancer Immunotherapy Grant.

1. Zinkernagel RM, Doherty PC (1974) Restriction of *in vitro* T cell-mediated cytotoxicity in lymphocytic choriomeningitis within a syngeneic or semiallogeneic system. *Nature* 248:701–702.
2. van der Merwe PA, Davis SJ (2003) Molecular interactions mediating T cell antigen recognition. *Annu Rev Immunol* 21:659–684.
3. Nikolich-Zugich J, Slifka MK, Messaoudi I (2004) The many important facets of T cell repertoire diversity. *Nat Rev Immunol* 4:123–132.
4. Moss PA, *et al.* (1991) Extensive conservation of α- and β-chains of the human T cell antigen receptor recognizing HLA-A2 and influenza A matrix peptide. *Proc Natl Acad Sci USA* 88:8987–8990.
5. Argaet VP, *et al.* (1994) Dominant selection of an invariant T cell antigen receptor in response to persistent infection by Epstein–Barr virus. *J Exp Med* 180:2335–2340.
6. Rudolph MG, Stanfield RL, Wilson IA (2006) How TCRs bind MHCs, peptides, and coreceptors. *Annu Rev Immunol* 24:419–466.
7. Sette A, *et al.* (1994) The relationship between class I binding affinity and immunogenicity of potential cytotoxic T cell epitopes. *J Immunol* 153:5586–5592.
8. Valmori D, *et al.* (2002) Vaccination with a Melan-A peptide selects an oligoclonal T cell population with increased functional avidity and tumor reactivity. *J Immunol* 168:4231–4240.
9. Kuball J, *et al.* (2005) Cooperation of human tumor-reactive CD4$^+$ and CD8$^+$ T cells after redirection of their specificity by a high-affinity p53A2.1-specific TCR. *Immunity* 22:117–129.
10. Le Gal FA, *et al.* (2005) Distinct structural TCR repertoires in naturally occurring versus vaccine-induced CD8$^+$ T cell responses to the tumor-specific antigen NY-ESO-1. *J Immunother* 28:252–257.
11. Baumgaertner P, *et al.* (2006) *Ex vivo* detectable human CD8 T cell responses to cancer-testis antigens. *Cancer Res* 66:1912–1916.
12. Derre L, *et al.* (2007) *In vivo* persistence of codominant human CD8$^+$ T cell clonotypes is not limited by replicative senescence or functional alteration. *J Immunol* 179:2368–2379.
13. Valmori D, *et al.* (2000) Naturally occurring human lymphocyte antigen-A2 restricted CD8$^+$ T cell response to the cancer testis antigen NY-ESO-1 in melanoma patients. *Cancer Res* 60:4499–4506.
14. Romero P, *et al.* (2001) CD8$^+$ T cell response to NY-ESO-1: Relative antigenicity and *in vitro* immunogenicity of natural and analogue sequences. *Clin Cancer Res* 7:766s–772s.
15. Chen JL, *et al.* (2005) Structural and kinetic basis for heightened immunogenicity of T cell vaccines. *J Exp Med* 201:1243–1255.
16. Zhong W, *et al.* (2007) CTL recognition of a protective immunodominant influenza A virus nucleoprotein epitope utilizes a highly restricted Vβ but diverse Vα repertoire: Functional and structural implications. *J Mol Biol* 372:535–548.
17. Dong T, *et al.* (2004) HIV-specific cytotoxic T cells from long-term survivors select a unique T cell receptor. *J Exp Med* 200:1547–1557.
18. Yokosuka T, *et al.* (2002) Predominant role of T cell receptor (TCR) α-chain in forming preimmune TCR repertoire revealed by clonal TCR reconstitution system. *J Exp Med* 195:991–1001.
19. Trautmann L, *et al.* (2002) Dominant TCR Vα usage by virus- and tumor-reactive T cells with wide affinity ranges for their specific antigens. *Eur J Immunol* 32:3181–3190.
20. Dietrich PY, *et al.* (2003) Prevalent role of TCR α-chain in the selection of the preimmune repertoire specific for a human tumor-associated self-antigen. *J Immunol* 170:5103–5109.
21. Miles JJ, *et al.* (2006) TCR α genes direct MHC restriction in the potent human T cell response to a class I-bound viral epitope. *J Immunol* 177:6804–6814.
22. Taubert R, Schwendemann J, Kyewski B (2007) Highly variable expression of tissue-restricted self-antigens in human thymus: Implications for self-tolerance and autoimmunity. *Eur J Immunol* 37:838–848.
23. Dietrich PY, *et al.* (2001) Melanoma patients respond to a cytotoxic T lymphocyte-defined self-peptide with diverse and nonoverlapping T cell receptor repertoires. *Cancer Res* 61:2047–2054.
24. Stewart-Jones GB, McMichael AJ, Bell JI, Stuart DI, Jones EY (2003) A structural basis for immunodominant human T cell receptor recognition. *Nat Immunol* 4:657–663.
25. Krogsgaard M, Davis MM (2005) How T cells ''see'' antigen. *Nat Immunol* 6:239–245.
26. Sami M, *et al.* (2007) Crystal structures of high-affinity human T cell receptors bound to peptide major histocompatibility complex reveal native diagonal binding geometry. *Protein Eng Des Sel* 20:397–403.
27. Gallimore A, Dumrese T, Hengartner H, Zinkernagel RM, Rammensee HG (1998) Protective immunity does not correlate with the hierarchy of virus-specific cytotoxic T cell responses to naturally processed peptides. *J Exp Med* 187:1647–1657.
28. Sali A, Blundell TL (1993) Comparative protein modelling by satisfaction of spatial restraints. *J Mol Biol* 234:779–815.

Supporting Information

Derré *et al.* 10.1073/pnas.0807954105

SI Text

In a few systems, strong biases in the T cell receptor (TCR) repertoire selection of antigen-specific T cells, resulting in the preferential usage of particular $\alpha\beta$ TCR combinations, have been reported (1–3). The human CTL response to influenza A matrix in individuals with HLA-A*0201 is characterized by prominent usage of the TCR-AV10.2-BV17 containing a conserved Arg–Ser–Ser sequence within the CDR3β regions (1, 3). Another example involves the T cell response to the EBNA3 antigen of Epstein–Barr virus (EBV) seen in HLA-B8-positive individuals whereby nearly all specific $CD8^+$ T cells use TCR-AV4.1-BV6.2 and share conserved CDR3 sequences (2). More recently, Gillespie *et al*. (4) described the preferential usage of AV15.1 and BV17 TCR, with striking sequence conservation throughout the hypervariable region, in a HLA-B*57-restricted immune response in HIV-1 infection.

Results. ***Naturally occurring NY-ESO-$1_{157–165}$-specific $CD8^+$ T cell responses display a preferential usage of BV1, BV8, and BV13TCRs.*** By using HLA-A2/NY-ESO-$1_{157–165}$ multimers in combination with mAbs directed against the variable region of TCR BV1, BV8, and BV13, we found that the majority of multimer$^+$ T cells expressed TCRs with these BV elements Fig. S1, in line with a recent report by Le Gal *et al*. (5). In patients LAU 50, LAU 155, LAU 156, and LAU 198, the proportion of NY-ESO-1-specific T cells bearing TCR BV1 was lower compared with cells expressing TCR BV8 and/or BV13 segments. BV8-positive cells were found predominantly in patient LAU 156, whereas most of the tumor-specific T cells of patient LAU 198 displayed the BV13 segment.

Analysis of distinct TCR BV1, BV8, and BV13 NY-ESO-1-reactive T cells by using clonotypic primers. The TCR BV and AV nomenclature used was according to Arden *et al.* (6) and Genevee *et al.* (7). To study the clonal composition of NY-ESO-1-specific T cell clones generated from patient LAU 50 (8), two distinct sets of primers specific for each clonotypic CDR3 sequence of these characterized T cell clones were designed: forward (Fwd) and reverse (Rev) (Fig. S2*A*). The sets designed for BV1 and BV13 T cell clonotypes were highly specific and allowed efficient clonotypic discrimination of each respective clone (Fig. S2 *B* and *D*). In contrast, all designed BV8 clonotypic primers displayed some degree of cross-reactivity among clonotypes 1–4 (Fig. S2*C*). In addition, BV8 clonotype-specific PCRs were clearly less efficient in identifying the different clonotypes because a large fraction of the performed PCRs (44%) gave a single positive product (+/− instead of +/+), and full clonotypic discrimination required extensive sequencing (Fig. S2*E*). Consistent with these results, sequence alignment and comparison of the four BV8 NY-ESO-1-specific T cell clonotypes revealed a high degree of homology in both the length and sequence of the CDR3β region (Fig. S2*B* and ref. 8).

Assessment of tumor cell killing by NY-ESO-1-specific T cell clones from patient LAU 50. Overall, all distinct T cell clonotypes efficiently recognized the NY-ESO-1 expressing melanoma cell lines Me 275 and Me 290, the former of which was autologous (i.e., derived from a metastasis of patient LAU 50). Consistent with the data obtained from peptide-pulsed T2 cells (see Fig. 3 of the main text), BV13-clono2 cells recognized tumor cells slightly less efficiently (Fig. S3).

Distinct NY-ESO-1-specific T cell clonotypes from patient LAU 155 exhibit similar functional avidity of antigen recognition. We compared the efficiency of peptide recognition by NY-ESO-1-specific T cell clonotypes isolated from another melanoma patient, LAU 155, by peptide titration killing assays on 17 representative T cell clones of defined TCR clonotypic sequences (Fig. S4). Most BV1-, BV8-, and BV13-derived clones killed T2 cells with an IC_{50} ranging widely between 10^{-10} and 10^{-8} M for the native and 2×10^{-11} and 10^{-9} M for the analog peptide, respectively. BV13 clonotypes displayed slightly superior peptide recognition compared with BV1 and BV8 clones, in line with their increased ability to recognized NY-ESO-1-expressing tumor cell lines (Me 275, Me 290) (data not shown). Altogether, these data further support the notion that T cells bearing three distinct sets of TCRs (either AVx/BV1, AV3/BV8, or AVx/BV13) shared similar avidity for antigen recognition, irrespectively of their BV usage.

Discussion. An important aspect is the functional antigen recognition and its relation to TCR sequence and structure. Our work was focused on dominant T cell clonotypes, which had expanded successfully *in vivo*. Therefore, it was particularly interesting to investigate whether their TCRs conferred efficient antigen recognition also *in vitro*, justifying the effort to generate a very large number of functional T cell clones. Indeed, they recognized and killed NY-ESO-1^+ tumor cells and peptide-pulsed T2 cells efficiently and with similar functional avidity, despite the usage of largely different TCRs. These data are consistent with our recent report (8) showing that in patient LAU 50, both BV8 and BV13 tumor-reactive clonotypes efficiently secreted effector mediators such as granzyme B, perforin, and IFN-γ, and killed tumor cells when tested directly *ex vivo* in a LiveCount assay (9). Altogether, these observations revealed that T cell clonotypes bearing molecularly defined distinct TCRs not only displayed full effector function but also killed target cells with similar antigen sensitivity, indicating that different TCR $\alpha\beta$ usage was not associated with different functional TCR avidity.

Another finding was that despite the relative diversification of the NY-ESO-1-specific TCR repertoire with the characterization of up to 12, 21, and 16 distinct BV1, BV8, and BV13 V(D)J junctional sequences, respectively (see Fig. 1 in the main text), the number of dominant NY-ESO-1-specific T cell clones found among individual melanoma patients was in fact rather limited. In patients LAU 50 and LAU 155, we, respectively, identified 10 and 6 distinct and codominant T cell clonotypes bearing BV1, BV8, and BV13 TCRs. Strikingly, we recently reported that the great majority of NY-ESO-1-specific T lymphocytes, in patient LAU 50, were composed of BV8 clonotypes 1 and 2 and of BV13 clonotypes 1 and 2 (8). Finally, NY-ESO-1/A*0201-specific T cell responses were dominated by a single dominant clone in patients LAU 156 and LAU 198, respectively. Collectively, our data indicate that similarly to our study on T cell responses against the immunodominant Melan-A/MART1 antigen (10), responses to NY-ESO-1 are also caused by selection and amplification of particular T cell clonotypes.

Materials and Methods. ***Patients, cell preparation, and flow cytometry.*** Peripheral blood mononuclear cells (PBMCs) were obtained by density centrifugation using Ficoll–Hypaque (Amersham Pharmacia) and cryopreserved in RPMI medium 1640 supplemented with 40% FCS and 10% DMSO (1×10^7 to 2×10^7 cells per vial). For peptide stimulation experiments, $CD8^+$ T lymphocytes were positively selected from PBMCs using anti-CD8-coated magnetic microbeads (Miltenyi Biotech), resulting in more than 90% $CD3^+CD8^+$ lymphocytes. Cells from the $CD8^{neg}$ fraction were irradiated (3,000 rad) and used as autologous antigen-presenting cells (APCs). $CD8^{pos}$-enriched lymphocytes (1×10^6 per well)

were stimulated with the NY-ESO-1 analog peptide (1 μM) and irradiated autologous APCs in 2 ml of RPMI medium 1640 containing 8% of human serum, 10 units/ml human recombinant IL-2 (hrIL-2; a gift from GlaxoSmithKline), and hrIL-7 (10 ng/ml; R&D Systems). A second round of peptide-specific stimulation was performed after 15 days, and cells were cultured for 15 additional days before HLA-A2/NY-ESO-1 multimer analysis. Synthesis of phycoerythrin (PE)- or allophycocyanin-labeled HLA-A*0201/peptide multimers was prepared as described in ref. 11 with NY-ESO-1 analog peptide 157–165 C165A (SLLMWITQA). Three-color stains were done with PE- or allophycocyanin-labeled HLA-A2/peptide multimers, FITC-conjugated anti-CD8 (Becton Dickinson), and PE-conjugated anti-TCR BV1, BV8, and BV13 (Beckman Coulter). Cells were first incubated with PE- or allophycocyanin-labeled multimers for 30 min at 4°C in PBS, 0.2% BSA, 50 μM EDTA, and then with appropriate antibodies (30 min, 4°C). Cells were washed once in the same buffer and immediately analyzed on a BD Vantage flow cytometer by using CellQuest software (Becton Dickinson).

Generation of T cell clones and functional cytolytic assays. Multimer^{pos} CD8^{pos} T cells were sorted in a FACSVantage SE machine (Becton Dickinson), cloned by limiting dilution, and expanded in RPMI medium 1640 supplemented with 8% human serum (HS), 150 units/ml recombinant human IL-2 (rIL-2; a gift from GlaxoSmithKline), 1 μg/ml phytohemagglutinin (PHA; Sodiag), and 1×10^6/ml irradiated allogeneic PBMC (3,000 rad) as feeder cells. A2/NY-ESO-1-multimer$^+$ T cell clones were expanded by periodic (every 15 days) restimulation in 24-well plates with PHA, irradiated feeder cells, and hrIL-2.

The functional avidity of antigen recognition was analyzed for *in vitro* generated T cell clones, isolated from patients LAU 50 and LAU 155, and bearing molecularly defined $\alpha\beta$ TCR clonotypes. Antigen recognition was assessed in a 4-h ^{51}Cr release assay by using radioactively labeled T2 target cells (1,000 cells per well; HLA-A2$^+$/TAP$^{-/-}$) pulsed with serial dilutions of the natural peptide residues 157–165 (SLLMWITQC) and the analog peptide with a C to A substitution at peptide position 9 for improved anchoring to HLA-A*0201 (12) before the addition of the different T cell clonotypes (100,000 cells per well). Unless otherwise specified, NY-ESO-1 peptides were preincubated for 1 h at room temperature with the disulfide-reducing agent Tris [2-carboxyethyl] phosphine (TCEP; 2 mM, Pierce Biotechnology) before being used to stimulate PBMCs or before functional assays. In the latter case, TCEP was further added during the assay at a final concentration of 500 μM. The specific antigen recognition lytic activity of the NY-ESO-1-specific T cell clonotypes was assessed against the melanoma cell lines Me 275 and Me 290 (HLA-A2$^+$/NY-ESO-1$^+$) and NA8-MEL (HLA-A2$^+$/NY-ESO-1$^-$). The percentage of specific lysis was calculated as $100 \times$ [(experimental $-$ spontaneous release)/(total $-$ spontaneous release)]. The relative antigenic activity of each peptide of the set of NY-ESO-1$_{157–165}$ single alanine-substituted peptide variants toward different T cell clonotypes was calculated as the [nM] 50% (EC_{50}) of the parental NY-ESO-1$_{157–165}$ nonapeptide (SLLMWITQC) divided by the [nM] 50% of index peptide.

TCR BV and AV repertoire analysis. Briefly, cDNA generated from NY-ESO-1^{pos} T cell clones was subjected to individual PCRs by using validated 5′-sense fluorescent-labeled primers specific for the V region of the β-chain subfamilies 1, 8, and 13 (BV1, BV8, and BV13), based on the nomenclature proposed by Arden *et al.* (6), and one 3′-antisense primer specific for the corresponding C gene segment (13). PCR products were then run on an automated sequencer in the presence of fluorescent size markers, and data analysis was performed with the Genescan analysis software (Applied Biosystems). We then subjected the cDNA of the TCR BV-identified NY-ESO-1-specific T cell clones to individual PCRs by using a set of validated 5′-sense primers specific for 33 V region of the α-chain (AV) subfamilies and one 3′-antisense primer specific for the corresponding C gene segment (7). TCR AV-AC and BV-BC PCR products were directly purified and sequenced (Fasteris).

Two distinct sets of primers (Metabion) specific for the CDR3 region of each identified BV1, BV8, and BV13 T cell clonotype from patient LAU 50 were validated and used for clonotyping PCR as described in ref. 8, (*i*) CDR3 clonotype forward and Cβ reverse, and (*ii*) BV subfamilies (BV1, BV8, or BV13) forward and CDR3 clonotype reverse as follows: BV1 clonotype 1, 5′-AGCGTAACAGGGACAGGGG-3′ and rev-5′-GCCCCCT-GTCCCTGTTACG-3′; BV1 clonotype 2, 5′-GTAGATG-GAAG CAATCAGCC-3′ and rev-5′-AAAATGCTGGGGCT-GATTGC-3′; BV8 clonotype 1, 5′-ACTTCTGTGCCAGC-CAACAG-3′ and rev-5′-AAAGCTTCAGTACCCCCCTG-3′; BV8 clonotype 2, 5′-ACTTCTGTGCCAGCAGTCTC-3′ and rev-5′-AAGCTTCAGTC CCCCCGAGA-3′; BV8 clonotype 3, 5′-GTTTGGGGGGCAATGAGCAG-3′ and rev-5′-GAACT-GCTCATTGCCCCCCA-3′; BV13 clonotype 1, 5′-GAA-CAGGGTTGGA CGGCTAC-3′ and rev-5′-GTAGCCGTC-CAACCCTGTTC-3′; BV13 clonotype 2, 5′-AGTTACG-TAGGGGGGAAGG-3′ and rev-5′-AGCCTTCCCCCC-TACGTAA-3′; and BV13 clonotype 3, 5′-GACACTATAAT-TCACCCCTCC-3′ and rev-5′-GGAGGGGTG AATTATAGT-GTC-3′.

Binding free energy calculations. To calculate the binding free energy contributions of each residue of the NY-ESO-1 peptide to the TCR–pMHC association, we chose the TCR BV13 clonotype 1 from LAU 155 and used the atomic coordinates of the highly related TCR AV23-BV13 (1G4) bound to NY-ESO-1$_{157–165}$/HLA-A*0201, retrieved from the Protein Data Bank (PDB ID code 2BNR) (14). Four TCR residues were mutated first, to generate a 3D model of the TCR BV13 clonotype 1 from LAU 155 (see Fig. 4 of the main text); Thr-95 and Ser-96 of the CDR3α were replaced by Gln and Thr, respectively, and the Asn-97 and Thr-98 of the CDR3β were replaced by Ala. The *in silico* amino acid substitutions were introduced into the reference TCR atomic coordinates by means of the Molecular Mechanics–Generalized Born Surface Area (15, 16) (MM-GBSA) approach for binding free energy estimation and decomposition. This method was used previously on a TCR-pMHC system and successfully reproduced the results of an experimental alanine scanning (16) as well as allowed a straightforward decomposition of the binding free energy into backbone and side-chain contributions for each residue as detailed in ref. 16. The averaged binding free energy contributions were calculated for all residues. All calculations were performed by using the CHARMM package (version c31b1) (17) and the CHARMM22 all-atoms force field (18). Contributions were averaged over a state of the art 1-ns MD simulation in explicit solvent, by using periodic boundary conditions and at constant pressure (1 atm) and temperature (300 K).

Computational TCR modeling. Homology models of the variable domain of the TCR bound to the SLLMWITQC peptide presented by HLA-A*0201 were built by using Modeler 6v2 (19), based on the 2BNR complex and other crystal structures of TCR from the Protein Data Bank. The 2BNR complex (14) was used as a structural template for TCR and pMHC homology modeling. From the available experimental structures of TCR or TCR–pMHC class I complexes, we selected the variable domains of 11 TCR (Vα and Vβ) as additional templates for the homology modeling: 1ao7, 1bd2, 1fo0, 1g6r, 1kb5, 1kj2, 1lp9, 1mi5, 1nfd, 1oga, and 2ckb. Lower-resolution redundant structures were excluded. Three unbound TCR Vα (1b88, 1i9e, and 1h5b) and two unbound TCR Vβ (1bec and 1ktk) structures were added to the templates list. The TCRVα structure 1934.4 was also used (20). Because the only complete TCR–pMHC template used was 2BNR, it is expected that the resulting models will have

a similar overall TCR orientation over pMHC, although small adjustments are possible. Once a homology model was obtained, each CDR loop was refined individually, while the rest of the complex, including the other CDR loops, remained unchanged. The loop modeling algorithm consists of a cycle of molecular dynamics simulations, combined with simulated annealing, optimizing the Modeler pseudoenergy function. Whenever possible, this function was improved by adding restraints specific to the nature of the CDR loop, derived from the rules given by Al-Lazikani *et al.* (21), where the identification of key amino acids defines limitations to the conformation space accessible to a CDR loop. The loops were refined one by one, in the following order, CDR2β, CDR1β, CDR2α, CDR1α, then both CDR3α and β were modeled at the same time. From each model that was obtained, we used CHARMM to calculate and decompose the binding free energy according to the MM-GBSA approach (15, 16), except that the quantities were not averaged along an MD simulation trajectory but calculated from the single structural model because of computing limitations. A 4 kcal/mol cutoff was applied to all residue contributions. Thus, all contributions that were larger than 4 kcal/mol or lower than -4 kcal/mol were set to 4 kcal/mol and -4 kcal/mol, respectively. This was done because values were calculated from a single structure and not averaged along a molecular dynamics simulation trajectory, leading to possible overestimation of favorable or unfavorable contributions. This cutoff was based on the maximum values that are usually observed by experimental alanine scanning (22). To assess the impact of the cutoff on the results, different values ranging from ± 3 kcal/mol to ± 6 kcal/mol were tested. No significant change in the calculated $\Delta G_{\alpha,\mathrm{bind}}$ and $\Delta G_{\beta,\mathrm{bind}}$ contributions were found, illustrating the robustness of the results (data not shown). Of note, because of its particularly long CDR3α and β, the BV13 clono1 from patient LAU 198 can be considered as an outlier and was removed from the calculations. In particular, the last step of the loop-modeling algorithm needs to estimate theoretically the conformation of a 23-aa loop, which is out of reach for the method.

1. Moss PA, *et al.* (1991) Extensive conservation of α- and β-chains of the human T-cell antigen receptor recognizing HLA-A2 and influenza A matrix peptide. *Proc Natl Acad Sci USA* 88:8987–8990.
2. Argaet VP, *et al.* (1994) Dominant selection of an invariant T cell antigen receptor in response to persistent infection by Epstein–Barr virus. *J Exp Med* 180:2335–2340.
3. Lehner PJ, *et al.* (1995) Human HLA-A0201-restricted cytotoxic T lymphocyte recognition of influenza A is dominated by T cells bearing the Vβ 17 gene segment. *J Exp Med* 181:79–91.
4. Gillespie GM, *et al.* (2006) Strong TCR conservation and altered T cell cross-reactivity characterize a B*57-restricted immune response in HIV-1 infection. *J Immunol* 177:3893–3902.
5. Le Gal FA, *et al.* (2005) Distinct structural TCR repertoires in naturally occurring versus vaccine-induced CD8$^+$ T-cell responses to the tumor-specific antigen NY-ESO-1. *J Immunother* 28:252–257.
6. Arden B, Clark SP, Kabelitz D, Mak TW (1995) Human T-cell receptor variable gene segment families. *Immunogenetics* 42:455–500.
7. Genevee C, *et al.* (1992) An experimentally validated panel of subfamily-specific oligonucleotide primers (Vα 1-w29/Vβ 1-w24) for the study of human T cell receptor variable V gene segment usage by polymerase chain reaction. *Eur J Immunol* 22:1261–1269.
8. Derre L, *et al.* (2007) *In vivo* persistence of codominant human CD8$^+$ T cell clonotypes is not limited by replicative senescence or functional alteration. *J Immunol* 179:2368–2379.
9. Devevre E, Romero P, Mahnke YD (2006) LiveCount assay: Concomitant measurement of cytolytic activity and phenotypic characterization of CD8$^+$ T-cells by flow cytometry. *J Immunol Methods* 311:31–46.
10. Speiser DE, *et al.* (2006) A novel approach to characterize clonality and differentiation of human melanoma-specific T cell responses: Spontaneous priming and efficient boosting by vaccination. *J Immunol* 177:1338–1348.
11. Altman JD, *et al.* (1996) Phenotypic analysis of antigen-specific T lymphocytes. *Science* 274:94–96.
12. Romero P, *et al.* (2001) CD8$^+$ T cell response to NY-ESO-1: Relative antigenicity and *in vitro* immunogenicity of natural and analogue sequences. *Clin Cancer Res* 7:766s–772s.
13. Roux E, *et al.* (1996) Analysis of T cell repopulation after allogeneic bone marrow transplantation: Significant differences between recipients of T cell-depleted and unmanipulated grafts. *Blood* 87:3984–3992.
14. Chen JL, *et al.* (2005) Structural and kinetic basis for heightened immunogenicity of T cell vaccines. *J Exp Med* 201:1243–1255.
15. Gohlke H, Kiel C, Case DA (2003) Insights into protein–protein binding by binding free energy calculation and free energy decomposition for the Ras–Raf and Ras–RalGDS complexes. *J Mol Biol* 330:891–913.
16. Zoete V, Michielin O (2007) Comparison between computational alanine scanning and per-residue binding free energy decomposition for protein–protein association using MM-GBSA: Application to the TCR–pMHC complex. *Proteins* 67:1026–1047.
17. Rufer N (2005) Molecular tracking of antigen-specific T-cell clones during immune responses. *Curr Opin Immunol* 17:441–447.
18. Rufer N, Reichenbach P, Romero P (2005) Methods for the *ex vivo* characterization of human CD8$^+$ T subsets based on gene expression and replicative history analysis. *Methods Mol Med* 109:265–284.
19. Sali A, Blundell TL (1993) Comparative protein modelling by satisfaction of spatial restraints. *J Mol Biol* 234:779–815.
20. Fields BA, *et al.* (1995) Crystal structure of the Vα domain of a T cell antigen receptor. *Science* 270:1821–1824.
21. Al-Lazikani B, Lesk AM, Chothia C (2000) Canonical structures for the hypervariable regions of T cell $\alpha\beta$ receptors. *J Mol Biol* 295:979–995.
22. Guerois R, Nielsen JE, Serrano L (2002) Predicting changes in the stability of proteins and protein complexes: A study of more than 1,000 mutations. *J Mol Biol* 320:369–387.

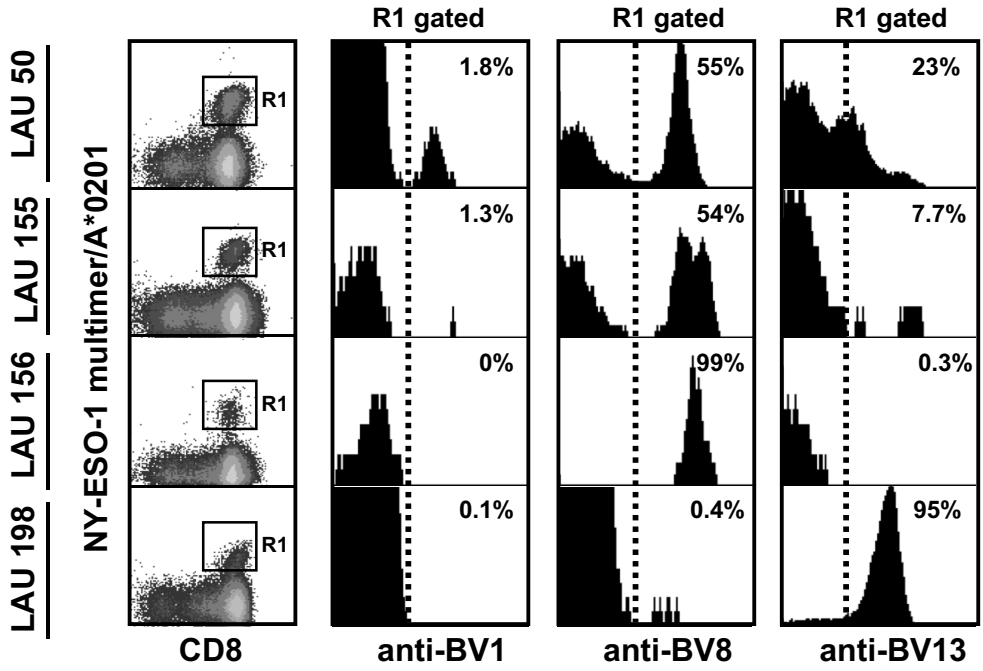

Fig. S1. TCR-BV usage of naturally occurring HLA-A*0201/NY-ESO-$1_{157–165}$ multimer$^+$ T cells in peptide-stimulated PBMCs from melanoma patients. Flow cytometry analysis of CD8$^+$multimer$^+$ T lymphocytes (R1) by using TCR BV1-, BV8-, and BV13-specific mAbs was performed. Data are shown as the percentage of BVx-expressing cells among CD8$^+$ multimer$^+$ T cells. Of note, only patients exhibiting the highest frequencies of NY-ESO-1-specific T cells are depicted (LAU 50, LAU 155, LAU 156, and LAU 198).

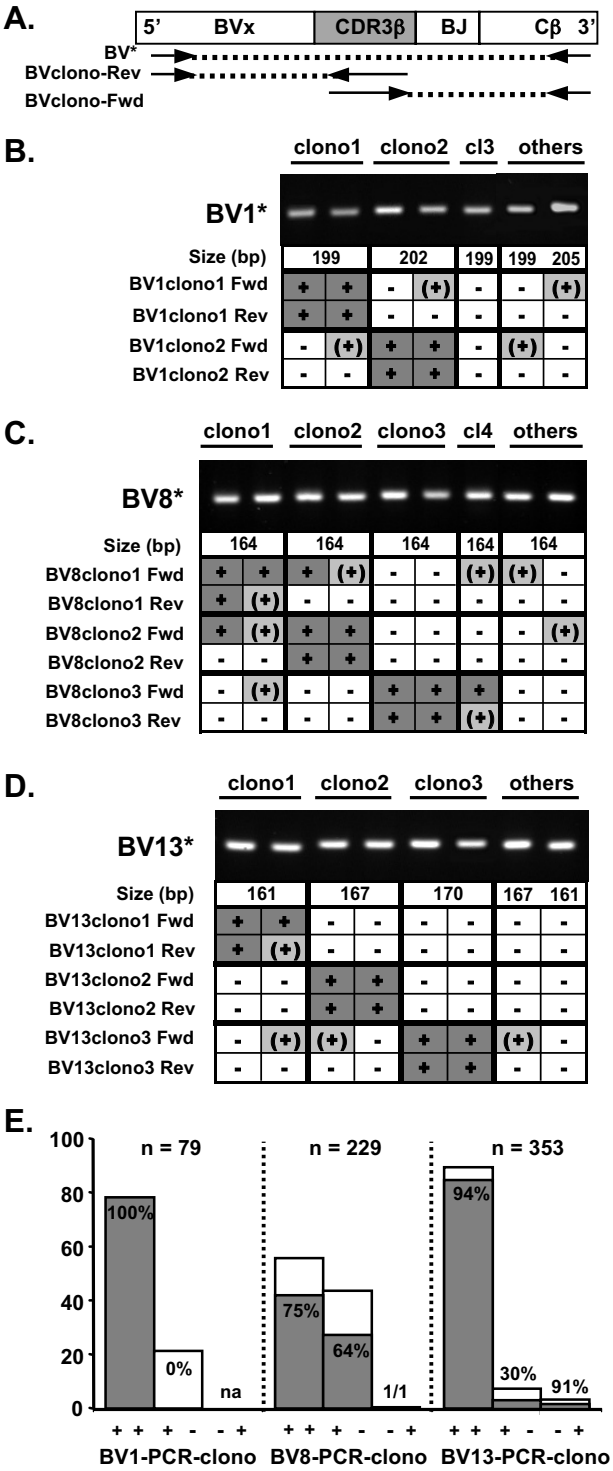

Fig. S2. Characterization of dominant T cell clones by clonotypic PCR and sequencing. (*A*) Unique primers corresponding to the *CDR3* gene segment of each identified TCR clonotype were designed and validated (see *SI Materials and Methods*). Two distinct sets of primers were used: (*i*) BVx forward–clonotype reverse (BVclono-Rev) and (*ii*) clonotype forward (BVclono-Fwd)–Cβ Reverse. (*B–D*) Clonotypic BV1 (*B*), BV8 (*C*), and BV13 (*D*) PCRs were performed on *in vitro* generated NY-ESO-1-specific T cell clones from patient LAU 50. The size for each amplified BV-CDR3-BC product is indicated (in base pairs). PCRs performed on distinct T cell clones bearing the same TCR clonotype are also depicted. (+) refers to low PCR expression levels. (*E*) The proportion (in percentage) of PCRs generating +/+ signals (positive PCR products with both BVclono-Fwd and BVclono-Rev sets of primers), +/− (positive PCR products with BVclono-Fwd only), and −/+ signals (positive PCR products with BVclono-Rev only). The percentage of BV1, BV8, and BV13 clonotypes confirmed by sequencing is depicted within each column and highlighted as gray bars. Of note, 64% of ''true'' BV8 T cell clonotypes gave a +/− PCR signal (false negatives). Conversely, 25% of +/+ PCR signals were not specific for the correct BV8 clonotype sequence (false positives). n represents the number of single T cell clones analyzed.

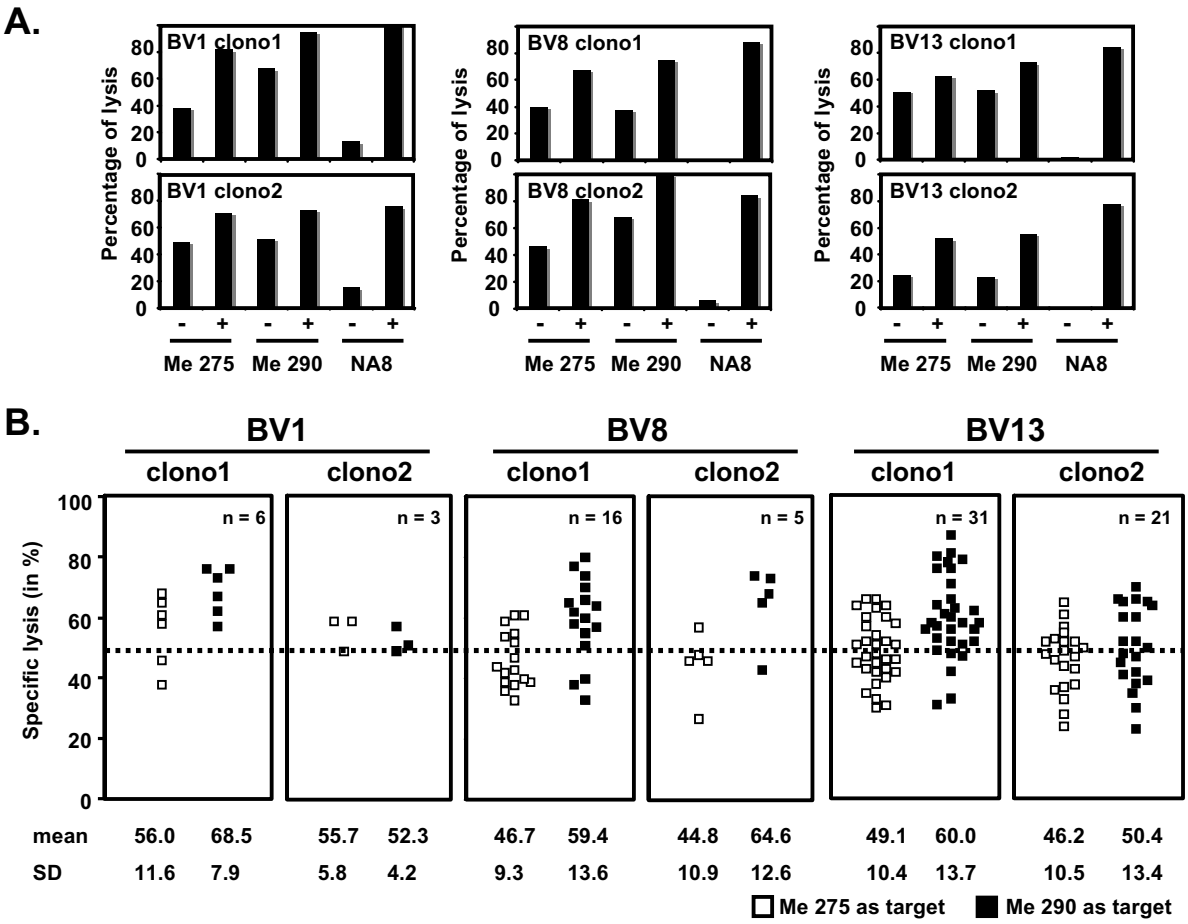

Fig. S3. Melanoma cell killing by T cell clones from patient LAU 50. (*A*) Tumor reactivity for the autologous melanoma cell lines Me 275 ($A2^+$/NY-ESO-1^+) and the allogeneic lines Me 290 ($A2^+$/NY-ESO-1^+) and NA8 ($A2^+$/NY-ESO-1^-) in the absence or presence of NY-ESO-$1_{157–165}$ analog peptide (1 μM) at an effector:target ratio of 30:1. Representative examples of percentage of specific lysis by BV1, BV8, and BV13 clonotypes 1 and 2 are depicted. (*B*) Complete set of data ($n = 82$ clones) representing the specific lysis of HLA-$A2^+$ tumor cells expressing NY-ESO-1 in the absence of peptide (30:1; effector:target ratio). Each data point represents the result of an individual clone. Mean ± SD values (in percentage) are shown.

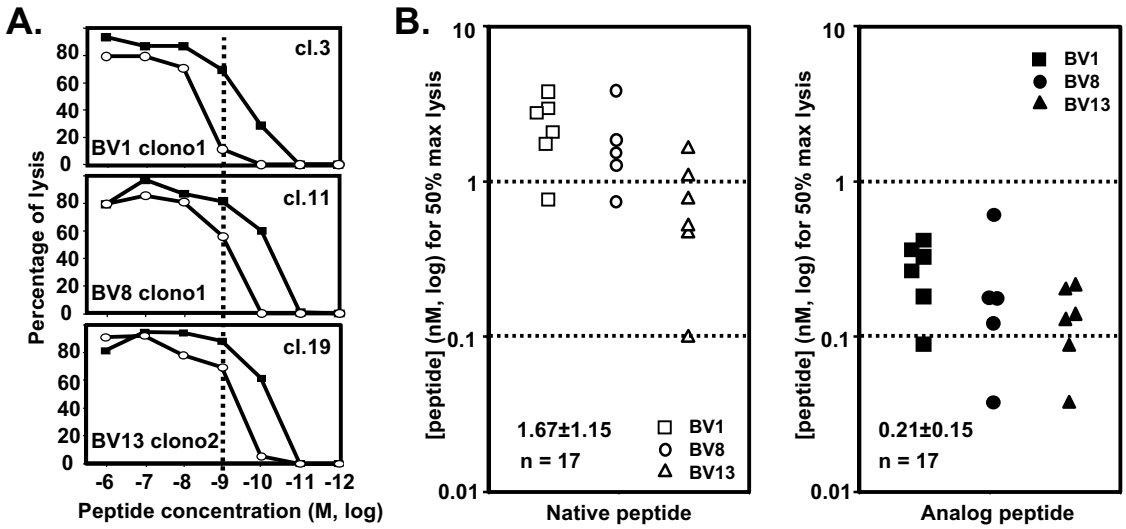

Fig. S4. Assessment of NY-ESO-1-peptide recognition of NY-ESO-1-specific T cell clones derived from patient LAU 155. (*A*) Representative examples of percentage of specific lysis by BV1, BV8, and BV13 clonotypes are depicted. The data show lysis of T2 cells loaded with varying concentrations of either native NY-ESO-1 peptide (open symbols) or its C165A substituted peptide analog (filled symbols). (*B*) Complete set of data ($n = 17$) representing the peptide concentration (either native or analog) required for 50% of maximum lysis. Each point represents the result of an individual clone. Mean ± SD values (nanomolar) are shown.